Sizing of a Propelled-Hopping System on the Moon

João Gambôa[1, *], Jasmine Rimani[1, 2], and Stéphanie Lizy-Destrez[1]

[1] *Institut Supérieur de l'Aéronautique et de l'Espace (ISAE-SUPAERO), Toulouse, France*

[2] *Politecnico di Torino (PoliTO), Torino, Italy*

[*] Corresponding author
Email: Joao-paulo.SILVA-GAMBOA@student.isae-supaero.fr

Abstract

Many space agencies foresee the return of humankind to the Moon in this decade, establishing a permanent human outpost that relies on in-situ resources and opening the gates to deep-space exploration. One of the envisioned locations for a human outpost is the lunar lava tubes. Those basaltic tunnels below the lunar surface are rich in materials and naturally shielded from radiation, micro-meteoroids, and temperature excursion. However, before venturing inside the tubes with a human mission, it would be fundamental to assess safety and map the underground caves using a robotic mission.

This study aims to size a thrust-propelled hopping system for the Moon and assess its feasibility for autonomous exploration and 3D mapping of lava tubes. The hopping-thrusting capabilities would help overcome the unknown terrain of lava tubes, as the system can perform short flights to avoid obstacles and navigate them, reaching areas farther from the entrance.

The sizing routine defines the hopping system's mass, power, thermal, and data budget. Then the focus is shifted to the performances and capabilities of the Guidance, Navigation, and Control (GNC) subsystem. The hopper relies on its optical payload to map and navigate the lava tubes. Therefore, a first mathematical model of the hopper has been developed to analyze the sensors needed for mapping and attitude control and their interactions with the control laws.

Subsequently, the exploration and mapping scenario will be detailed, along with the control laws and path-planning algorithms used to solve it. The GNC system will allow the hopper to localize itself, compute its path, avoid obstacles, and control its movement.

Therefore, the paper will first detail the system engineering study performed on the lava tube mission. The mission's primary objectives, requirements, and concept of operations will then be presented. Then the main trade-off at the subsystem level will be addressed. After, the main sizing rules for the hopper will be analyzed in detail. Eventually, an in-depth analysis of the GNC system will be proposed.

Keywords: Moon Hopper, Lava Tubes, Space system, Motion Planning, Nonlinear Programming, Hopping Trajectory Optimization

1. Introduction

Becoming a multi-planetary species is one of the goals for the XXI century, and it involves further developing human exploration beyond Earth and the Moon. Several projects have been envisioned to advance our technology and achieve this aim by the end of the decade. For example, the Lunar Gateway is a planned small space station in lunar orbit, intended to serve as a communication hub, science laboratory, and short-term habitation for astronauts. This hub can serve as a site for repairs and logistics support, and as a refueling depot between long journeys to the Moon and beyond [1].

The Lunar Gateway would support multiple trips to the Moon, aiming to utilize in-situ resources, support lunar exploration, and enable science endeavors. As a possible target of these future science missions, the lunar lava tubes emerge as an environment of interest, given that they can shelter the human outpost from the dangers of outer space, such as radiation, temperature amplitude, and micrometeoroids, while being close to essential resources for a human settlement, such as helium and hydrogen [2]. Lunar lava tubes were theorized in the early '70s [3] and have been observed from orbit [4]. However, those underground tunnels are still an unexplored maze.

Therefore, a robotic mission is envisioned to map these lava tubes and assess the environment's habitability and safety for humans. However, very little is known about the morphology and challenges awaiting in these basaltic tunnels. There are some estimations of possible depth and length [4]. However, a deeper investigation is needed. Several configurations have been proposed for the lava tube mission in [1], [5]–[7].

However, the current systems designed exclusively for the exploration of moon lava tubes, such as Daedalus [8] and SphereX [1], may not provide sufficient object traversability in environments where obstacle sizes are unknown. In particular, the Daedalus system lacks a propulsion system, so its obstacle-traversability is limited to a certain obstacle height. On the other hand, the Arizona hopper is a system that has limited autonomy [9].

This project proposes a lunar-propelled hopper with a hybrid mobility system: a wheeled system for traversing normal terrain and a propulsive system for overcoming larger obstacles. Beyond the skylight area, the lava tube terrain should be almost flat, as expected from basaltic terrain [10]. Therefore, a wheeled system would be perfect for traversing rapidly through a basaltic terrain.

The proposed system may complement the architectures in [1], [5]–[7] by considering a swarm of robots with complementary capabilities.

The lunar-propelled hopper's overall design is driven not only by the payload but also by its innovative mobility system. Therefore, the study addresses the hopper's preliminary sizing, identifies its subsystems, and quantifies the overall mass, power, and data budgets.

The focus is then shifted to the Guidance, Navigation, and Control (GNC) subsystem's performance and capabilities. In this part, a mathematical model describing the hopper's movement, based on an analogy with a missile trajectory, is first defined. Afterward, the trajectory is optimized. For optimization, a method is proposed based on the Interior Point OPTimizer in the *GEKKO* Python library [11], following the methodology presented in [12].

The remaining of the paper will be organized as follows: Section 2 analyses the methods employed in the hopper design and the mathematical background behind the mobility capabilities analysis, Section 3 would present the main results for the hopper trajectory design and system sizing, Section 4 would wrap up with the main outcomes of the paper, and it would briefly illustrate the main envisioned future works on the paper.

2. Methods and Materials

2.1 Lunar Hopper Design

A good preliminary sizing of mass and power is fundamental for assessing the feasibility and performance of the studied system. The system

design variables are valuable inputs to the dynamic model and are used in motion-planning simulations. During the system design, different mission constraints and requirements are analyzed. The most impactful ones for the lunar hopper are:

- According to [6], the system may need to venture up to 200 m inside the lunar lava tube. With a constraint of maximum communication between rovers of 80 m [1], it can be assumed that three systems can be enough to cover one direction of the lunar lava tube, and four can be lowered to have redundancy.
- Furthermore, if the system needs to be lowered by the robot crane studied during [7], [13], a maximum weight limit of 30 kg should be respected.
- Moreover, to not contaminate the lava tubes terrain, the propellant chosen is the LMP-103S, a replacement of hydrazine developed by the Swedish Company *Eurenco Bofors AB* [14], also used in [1]. This propellant has a specific impulse, I_{sp} of 243 s.

2.1.1 System sizing

The hopper design is based on a preliminary estimation of the mass and power of each subsystem. This is needed to determine the mission active phases and recharge phases, while also giving insight into the exploring and mapping scenario and the components required for the attitude control, driven by the sizing of the GNC capabilities.

The methodology presented in this paper for the design of the subsystems' power and mass is based on [15]. Throughout this project, the total mass of the hopper will be denoted by $m_{total,}$ and this mass will be broken into three primary mass components. These components are defined as dry mass, payload mass, and propellant mass, such that $m_{total} = m_{dry} + m_{pl} + m_{propellant.}$ (1)

The inertial mass denoted by m_{inert} is given by

$$m_{inert} = m_{dry} + m_{pl.} \quad (2)$$

According to [15], if each subsystem mass can be calculated, then the total mass is given by the sum of each subsystem mass. Each subsystem's mass, on the other hand, is a function of the dry mass. For example, the heavier the vehicle, the more mass the propulsion subsystem needs. Higher structural strength is also required as vehicle mass increases, thereby increasing structural mass. This can be expressed by equation 3, where the subsystem mass is required for dry mass calculations.

$$\begin{cases} m_{total} = f(m_{subsystem1}, m_{subsystem2}, \ldots), \\ m_{subsystem} = f(m_{dry}, a, b, \ldots). \end{cases} \quad (3)$$

Therefore, to determine the total mass of the subsystem, the total mass should be estimated, and then, using available mass-estimating relationships —for example, for manned landers [15] [16] and satellites [17] —the subsystem's mass is calculated. The hopper identified subsystems are summarized in Table 1.

Table 1: *Definitions of subsystems in the sizing methodology, based on [15]*

Subsystem	Sub-sub systems included	Purpose/Description
Payload	Sensors, Cameras	To Produce a 3D map of the lava tubes,
Structural	Landing legs, Main Body with components	Connect and support other mass components Enable the vehicle's landing on the surface
Propulsion	Propellant tanks,engines, propellant	Generate thrust for control and stability of the vehicle while hopping.
Power	Battery, electrical system	Ensure that the other systems have access to electricity.
Wheeled	Legs, Motors	Navigate the basaltic terrain in the lunar lava tube, traversing obstacles
Telemetry, Tracking and Command TT&C	Communications,control system	To relay the 3D map to Earth
On-board Processing	Main computer, GNC computer, displays, interfaces	Determine the position of the hopper. On-board decisions. Keep the system operational
Thermal	Thermal protection system (TPS)	To maintain the temperature of the system
Other	-	Other unidentified components that are necessary

The payload is the first subsystem to be sized, since the initial estimate of the total mass is the payload's mass.

The hopper must have a LiDAR system, essential to map the environment, a *Fisheye* to produce images inside the lunar lava tubes,

together with LED lighting, necessary to illuminate the environment for the camera. A gyroscope and accelerometer (*XSENS*) are essential to determine the acceleration and attitude of the hopper. A thermometer, to evaluate the on-board temperature, and a radiation dosimeter. Finally, a main onboard computer is needed as the hopper's main brain, while a navigation unit would handle the computational load of the GNC system. Table 2 resumes the mass and power needed for each component.

Table 2: *Payload components, based on [2]*

Sensors	Mass (kg)	Consumption (W)
LiDAR	1.3	12
Fisheye Camera	1.6	2.6
LED lightning	0.01	3.5
Gyroscope and Accelerometer	0.055	0.52
Thermometer	0.1	1
Radiation Dosimeter	0.1	1
Main Onboard Computer	0.055	0.9
Main Navigation Unit	0.055	0.9
Total	3.275	22.42

Based on this table and knowing that, according to [18], the mass of the payload for a surface planetary surface vehicle commonly represents about 8% to 13% of the total mass, the total mass can be estimated as:

$$m_{total} = m_{payload}/payload(\%). \quad (4)$$

This will be the initial guess used to calculate the mass of each subsystem.

For the propulsion subsystem, the propellant mass must first be defined. This will be sized based on the percentage of the total mass the hopper will need for one hop and the number of hops the system will perform. The mass of propellant ($m_{propellant}$) is therefore given by

$$m_{total} - m_{total}(1 - \frac{m_{hop}}{m_{total}})^{\lceil \frac{D}{R} \rceil}. \quad (5)$$

Where m_{hop}/m_{total} denotes the mass of the propellant out of the total mass that is needed to do one hop. D denotes the distance covered by the hopper in meters, and R represents the range the hopper can cover in one hop, in meters. The operator $\lceil\ \rceil$ denotes the ceiling function. According to [19], the equations that define the propulsion system are given by:

$$m_{Eng} = \frac{1}{10} T_{max}^{\frac{2}{3}}, \quad (6)$$

$$m_{Tank} = \frac{2}{3} m_{propellant}^{\frac{2}{3}}, \quad (7)$$

$$m_{propulsion} = 1.1(m_{Eng} + m_{Tank} + m_{propellant}). \quad (8)$$

Where m_{Eng} is the mass of the engine, m_{Tank} is the mass of the tank, $m_{propellant}$ is the mass of propellant needed, and $m_{propulsion}$ is the total mass of the propulsion system. The factor of 1.1 represents a 10% safe margin for the subsystem. T_{max} is the maximum thrust, which will be sized according to the equations.

$$T_{max} = twr \cdot W_0, \quad (9)$$

$$W_0 = m_{total} \cdot g_m. \quad (10)$$

Where twr denotes the Thrust-to-weight ratio, W_0 denotes the initial mass, and g_m the moon's gravity.

According to [19], the equation that gives the structural mass as a function of the total mass of the hopper is given by

$$m_{struc} = 1.1 \cdot \frac{3}{20} m_{total}. \quad (11)$$

The power system is sized to the payload's power requirements. According to [17], the payload's power represents 22% of the total power. Therefore, the total mass of the power subsystem is given by

$$m_{power} = 1.1 \cdot \frac{P_{payload}/0.22}{\rho_{Batteries}} \cdot T_{ap} \quad (12)$$

Where $P_{payload}$ is around 23 W, as shown in Table 2. $\rho_{Batteries}$ is the specific energy of the batteries. It will be assumed that the system will use Li-ion batteries with a specific energy of about 100 Wh kg^{-1} [18]. The factor of 1.1 again denotes the safety margin.

T_{ap} denotes the time of the active phase, a design-imposed limit. As stated before, the project aims for a compact design and multiple robots collaborating, with a maximum mass of 30 kg. Therefore, the mission duration had to be a value that respected a mission of this type. Therefore, an active phase of 2 hours was assumed.

The wheeled mobility subsystem is defined from a statistical analysis of similar systems, as shown in:

$$m_{wheeled} = 1.1 \cdot 0.17 \cdot m_{dry}. \quad (13)$$

The telemetry, tracking, and command (TT&C), on-board processing, and thermal subsystems are given as a percentage of the total dry mass. All the harnesses and mechanisms are considered as "other". The [17] presents the weight of these subsystems as a percentage of the dry mass for various planetary spacecrafts. Therefore, the following equations were considered:

$$m_{TT\&C} = 1.1 \cdot 0.07 \cdot m_{dry}, \quad (14)$$

$$m_{On-boardProc} = 1.1 \cdot 0.04 \cdot m_{dry}, \quad (15)$$

$$m_{Thermal} = 1.1 \cdot 0.06 \cdot m_{dry}, \quad (16)$$

$$m_{other} = 1.1 \cdot 0.04 \cdot m_{dry}. \quad (17)$$

For these equations, a safety margin of 10% was also identified following [20]. Therefore, the *total given by the sum of the mass of the subsystems is given by the sum of the results from equation 8, and equations 11 to 17,* and the mass of the payload, shown in table 2. This can also be expressed by the equation

$$m_{total} = \sum m_{subsystem}. \quad (18)$$

In conclusion, to apply this method, all the parameters that are needed for each of the equations of the subsystems must first be defined. These parameters are as follows.

$$[\frac{m_{prop-hop}}{m_{total}}, D_{covered}, R_{hop}, twr] \quad (19)$$

Then, the value of the m_{total} must be calculated, given by equations 4 and 18 for each value of the payload percentage defined within a certain range. For each of these iterations, it must be checked if convergence was achieved, meaning if the difference between the two values of m_{total} is zero. If it is, then the system sizing is successful and the initial *total* is correct.

Regarding the power budget, it is assumed that the payload accounts for 22% of the hopper's total power, as reported in [17]. Therefore, the total power required can be estimated with the following equation.

$$P_{total} = P_{payload}/0.22. \quad (20)$$

Yielding a result of around 102 W.

2.1.2 CAD

Taking all this into account, a computer-aided design (CAD) concept was done using *SOLIDWORKS*, in order to correctly visualize the system. This can be seen in Figure 1.

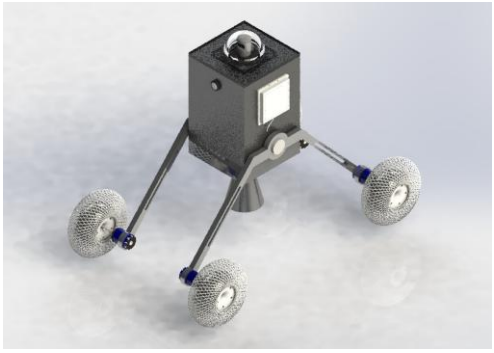

Figure 1: *Concept design of the hopper*

To control this hopper in the Z axis, a set of 2 reaction wheels must be used, one on each side, in order to have symmetry and better control.

In Figure 1, the fisheye camera can be seen in the front, with the LiDAR on top of the hopper, inside a cover. Three patch antennas are on the outside of the hopper, used for communications.

According to [8], the obstacles in the lava tube range from 99.636 mm to 2.344 mm. Therefore, a diameter of 180 mm was chosen for the wheels, considering that the hopper can transverse an obstacle with a size of half the wheel's diameter. Moreover, flexible wheels were also chosen, given that they have the ability to provide better grip on soft soils than rigid wheels of comparable diameter. This was viewed as a means to get a bigger wheel performance with a smaller wheel. [21].

2.2 Mathematical Model

The movement of the hopper will be designed by analogy with the trajectory of a missile, based on the assumption that a ballistic trajectory performed by the hopper is similar to that of a ballistic missile.

Throughout this paper, the axes will be oriented so that the y-axis is the vertical coordinate, the x-axis is the horizontal axis, and the z-axis points out of the page*, as shown in Figure* 2. The definitions of the angles present in Figure 2 will be used

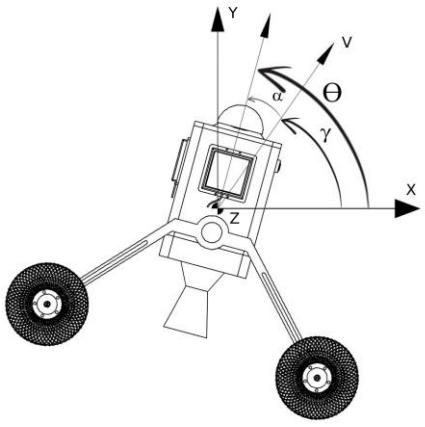

Figure 2: *Overview of the angles that define the movement*

In this figure, the angle α is the angle of attack, a measure of how the hopper is oriented relative to the velocity vector, being the angle between the upward axis and the velocity. The angle γ is a measure of the direction of travel relative to the inertial space, meaning the angle between the hopper velocity vector and the inertial reference. Finally, the angle θ, given by the sum of α and γ, *defines the orientation of the hopper relative to the inertial space and is the angle between the inertial reference and the hopper's upward* axis. [22]

According to [23], the equations of motion (EOM) that govern a missile in 3Dof are as follows

$$\dot{y} = V\sin(\gamma); \tag{22}$$

$$\dot{V} = \frac{T}{m}\cos(\alpha) - g_m\sin(\gamma); \tag{23}$$

$$\dot{\gamma} = \frac{T}{mV}\sin(\alpha) - \frac{g_m}{V}\cos(\gamma); \tag{24}$$

$$\theta = \alpha + \gamma. \tag{25}$$

Where V is the velocity of the hopper, as shown in Figure 2, m is the mass of the system, and g is the gravitational acceleration on the Moon, given by 1.625 m/s^2. T is the thrust given by the motor, which can also be described with the equation:

$$T = I_{sp}\dot{m}g_0 \tag{26}$$

Where I_{sp} is the specific impulse of the motor, in seconds, the $\dot{m}$ is the mass flow rate of the nozzle, and g_0 is standard gravity, equal to 9.81 m/s ^{2}.

According to [22], the equation that governs the pitch angle of the hopper can be modeled as:

$$\ddot{\theta} = \frac{M_{rw}}{J_Z}. \tag{27}$$

Where M_{rw} is the moment from the reaction wheels and J_Z is the moment of inertia of the hopper in the *z-axis*.

The mass of the hopper also changes according to the equation.

$$m = -\dot{m} \tag{28}$$

Where $\dot{m}$ is the mass flow rate.

Equations (21 to 28) define the complete system of equations that govern the motion of the hopper. Therefore, it can be concluded that for this system, the hopper will be controlled based on two inputs, the mass flow rate ($\dot{m}$) and the moment from the reaction wheels (M_{rw}).

2.3 Description of the trajectory

The ballistic trajectory of a single hop can be broken down into three phases: Ascent Phase, Ballistic Phase, and Landing Phase.

In the first phase, the ascent phase, the flight path angle will increase from 90º to a desired angle to achieve a ballistic trajectory over a certain distance. During this phase, the reaction wheel's moment must change the flight path angle. In this phase, the engine is turned on. To consume the least amount of fuel, this phase must be performed in a bang-bang optimal manner, with the mass flow rate maximized, thereby maximizing thrust during this ascent phase.

For the second phase, the ballistic phase, the engine is turned off. In this part of the trajectory, the vehicle follows a pure ballistic path as the reaction wheels begin orienting it and preparing it for the landing stage.

For the third phase, the engine will be turned on and, based on the optimal bang-bang solution, the thrust will be maximum, such that the vertical velocity in the end is reduced.

2.4 Description of the optimization problem

Therefore, this project aims to understand how to maximize the distance traveled while minimizing propellant use, or equivalently, maximizing the final mass. In this scope, the optimization problem can be formalized as a nonlinear programming problem (NLP) as follows:

Minimize:

$$J = -m(t_f) \quad \text{Objective function} \tag{29}$$

Subject to:

$$\begin{aligned} \dot{X} &= f(t, X, U) && \text{EOM} \\ X &= [x, y, V, \gamma, \dot{\theta}, \theta, m] && \text{state variables} \\ U &= [\dot{m}, M_{rw}] && \text{control variables} \end{aligned} \tag{30}$$

For this problem, the initial conditions are specified as:

$$\begin{cases} t_0 = 0; \\ x(t_0) = 0; \\ y(t_0) = 0; \\ V(t_0) = 0; \\ \gamma(t_0) = \pi/2; \\ \dot{\theta}(t_0) = 0; \\ \theta(t_0) = \pi/2; \\ m(t_0) = m_0. \end{cases} \tag{31}$$

As for the final conditions, it can be noted that for the hopper to be stable when landing, it must land oriented upwards, meaning the angle θ in the end must be equal to $\pi/2$. Moreover, it will be considered that the vertical velocity in the end must be, in absolute value, less than or equal to 3 m/s, assuming that this velocity is small enough to be supported by the hopper's wheels. This value is consistent with previous studies on preliminary lander sizing [24]. It was also assumed that the hopper's final horizontal velocity would be 1 m/s, in accordance with previous studies [25].

The hopper must also land at a desired distance, equal to the final value of x_f, which must be an input to the algorithm. Therefore, the final conditions are as follows:

$$\begin{cases} t_f = free; \\ x(t_f) = x_f; \\ y(t_f) = 0; \\ |V_y(t_f)| \leq 3m/s; \\ |V_x(t_f)| \leq 1m/s; \\ \gamma(t_f) = free; \\ \dot{\theta}(t_f) = 0; \\ \theta(t_f) = \pi/2; \\ m(t_f) = free \end{cases} \quad (32)$$

According to [17], the moment from a reaction wheel has a maximum absolute value of 1 N·m. The mass flow rate must also be sized such that its value is less than a value obtained with the thrust-to-weight ratio (*twr*). Therefore, for the input variables, the following restrictions are considered:

$$\begin{cases} -1/J_Z \leq M_{rw}/J_Z \leq 1/J_Z; \\ 0 \leq \dot{m} \leq (twr \cdot m_{total} \cdot g_m)/(Isp \cdot g_0). \end{cases} \quad (3$$

The *twr* ratio must be greater than 1 to ensure the hopper rises above the ground.

2.5 Numerical Solution

The gradient-based optimization approach was used to solve the optimization problem, based on previous work done [12]. The problem is formulated as a continuous-time optimal control problem and then translated into a nonlinear programming (NLP) problem. After that, gradient-based optimizers like IPOPT are used to solve the NLP. To solve this problem, the library *GEKKO* [11] was chosen, due to its simple syntax, available documentation, and examples. This library is powerful in solving big and complex problems, such as [26]. However, for this algorithm, an initial guess is required.

2.5.1 Initial Guess

As stated in section 2.4, the final vertical velocity must be, in absolute value, less than 3 m/s. Therefore, to minimize the amount of propellant used, it will be considered that the movement can be done without the landing phase stated in section 2.3. For that reason, the trajectory will be sized based on the assumption that the vertical velocity at the end of the ballistic phase (see figure 3) is, in absolute value, equal to 2.5 m/s, a lower value than the 3 m/s in order to have a safety margin.

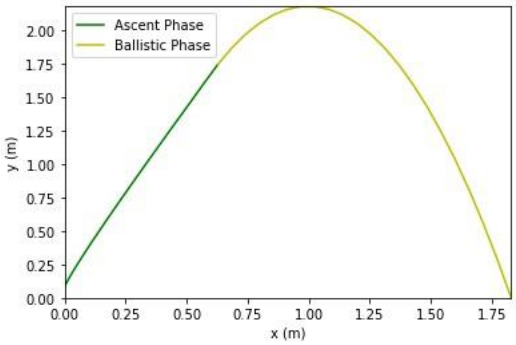

Figure 3: *Trajectory of the hopper, without the Landing Phase.*

To calculate this initial guess, the trajectory must first be decomposed into two stages: the ascent phase and the ballistic phase, each described by equations.

First, the node at the end of the Ascent Phase will be denoted with the subscript *bal* (as in ballistic). Meaning, at the end of this phase, the trajectory will be ballistic. Therefore, the following can be denoted as:

$$y_{bal}, V_{bal}, t_{bal}, \gamma_{bal}. \quad (34)$$

When referring to the coordinate y, the velocity, the time at which it is achieved, and the flight path angle at the end of the ascent phase. On the other hand, the subscript *f* (as in final) denotes the node at the end of the Ballistic Phase. Therefore, it can be written

$$y_f, V_f, t_f, \gamma_f. \quad (35)$$

At the end of the ballistic trajectory, a vertical velocity of -2.5 m/s (negative due to the fact that the velocity vector is pointing downwards, in the negative y direction) is needed. The equation that denotes this velocity is given by

$$V_{y_f} = -2.5 = V_{bal}\sin(\gamma_{bal}) - g_m(t_f - t_{bal}). \quad (36)$$

Where g_m denotes the moon gravity acceleration and the term $(t_f - t_{bal})$ denotes the time of the ballistic trajectory. Based on this equation, it can be understood that the t_f must be defined as a function of the initial conditions of the ballistic phase. This can be easily done by using the equations of a projectile motion. Starting from the equation that defines the vertical motion applied for this system, and knowing that $y(t_f) = 0$, one can conclude that

$$t_f = \frac{V_{bal}\sin(\gamma_{bal})}{g_m}\left(1+\sqrt{1+\frac{2y_{bal}g_m}{(V_{bal}\sin(\gamma_{bal}))^2}}\right)+t_{bal}. \quad (37)$$

The equations 36 and 37 define the ballistic phase. Two equations for the Ascent Phase are now needed.

Assuming a bang bang approach, the thrust in this initial ascent phase is equal to T_{max}, meaning equal to $twr \cdot m_{total} \cdot g_m$, according to equation 33. It is assumed that the hopper is aligned with the trajectory, meaning $\alpha = 0$. If these assumptions to the equations described in the section 2.2 are applied the following equations can be written:

$$V_{bal} = \int_0^{t_{bal}} twr \cdot g_m - g_m \sin(\gamma(t))\, dt; \quad (38)$$

$$y_{bal} = \int_0^{t_{bal}} V\sin(\gamma(t))dt = \int_0^{t_{bal}} \left(\int_0^t twr \cdot g_m - g_m \sin(\gamma(t))\, dt\right)\sin(\gamma(t))dt. \quad (39)$$

In order to complete the system, an initial estimation for the function $\gamma(t)$ is needed. By lookin at figure 3, it can be estimated that the evolution of $\gamma(t)$ during the ascent phase can be parabolic. This function must also have the proprieties $\gamma(0) = \gamma(t_0) = \pi/2$ and $\gamma(t_{bal}) = \gamma_{bal}$. For that reason, it will be assumed that

$$\gamma(t) = \gamma_{bal} + \frac{\pi/2 - \gamma_{bal}}{t_{bal}^2}(t - t_{bal})^2. \quad (40)$$

The last equation that completes the system is given by the range of the hop, and combines both the ascent and ballistic phase. To solve the equations, the range of the value of x_f must be given. The equation is as follows:

$$x_f = \int_0^{t_{bal}} \left(\int_0^t twr \cdot g_m - g_m \sin(\gamma(t))\, dt\right)\cos\gamma(t)dt + V_{bal}\cos(\gamma_{bal})(t_f - t_{bal}). \quad (41)$$

Therefore, 5 equations are considered, 36 to 39 and 41 and 5 unknowns $v_{bal}, y_{bal}, t_f, t_{bal}, \gamma_{bal}$ therefore closing the system. This was solved using *Python* and, in particular, the libraries *numpy* [27] and *scipy* [28].

2.5.2 *Optimization*

After calculating the initial guess as stated in the previous section, an optimization can be done using *GEKKO* [29]. To use this library, all the variables must first be initialized to the values stated in 31. The equations are then written with the *GEKKO* library syntax. The control variables, which also need an initial value, were initialized as

$$\begin{cases} \dot{m} = \dot{m}_{max}; \\ M_{rw} = 0. \end{cases} \quad (42)$$

Regarding the constraints used, the library has the options of denoting hard and soft constraints. The

library offers three main types of constraints: fixing the final value, minimizing the difference between the reference and a certain value, and having a certain value under a reference. For constraints essential to the mission's success, harder constraints were necessary. For example, the final vertical velocity must be, in absolute value, under 3 m/s; otherwise, the hopper might not survive the jump. The horizontal velocity must also be a hard constraint.

On the other hand, the final distance is a softer constraint. If the value of $x(t_f)$ is close to x_f, but not equal, then the hopper still survives, and the mission can continue. For the same reason, a softer constraint is defined for the final angle θ, which must be close to 90° in order for the hopper to land in the upward position. In summary, the following constraints were defined:

$$\begin{aligned} min \quad & -m(t_f) + (x(t_f) - x_f)^2 + (\theta(t_f) - \pi/2)^2; \\ & V(t_f)\sin(\gamma(t_f)) \leq 3m/s; \\ & V(t_f)\cos(\gamma(t_f)) \leq 1m/s; \\ & y(t_f) \leq 0. \end{aligned}$$
$$t \qquad (43)$$

The trajectory must always maximize the final mass, therefore the first equation in 43 is considered. Finally, the final value of y must be less than 0 making sure the trajectory is done completely. The IPOPT solver was used.

3. Results and Discussion

3.1 Final Design

The methodology applied for the subsystem sizing is mentioned in section 2.1. For the code, the parameters stated in equation 19 were defined as follows:

$$\begin{cases} \frac{m_{prop-hop}}{m_{total}} = 0.0022; \\ D_{covered} = 200\,m; \\ R_{hop} = 3.2\,m; \\ twr = 1.3. \end{cases} \qquad (44)$$

The value of $m_{prop-hop}/m_{total}$ is taken as 0.0022, as described in 3.2. According to [6], the system should venture 200 meters inside the cave. For this reason, the variable $D_{covered}$ is considered to be 200 m. The maximum range of the hop is 3.2 meters, as stated in 3.2. Moreover, the value of twr is set to 1.3, obtained by trial and error as stated in 3.2. From these inputs, the difference between the initial guess for the mass, calculated from equation 4, and the mass obtained with equation 18 as a function of the payload percentage can be plotted, as shown in Figure 4.

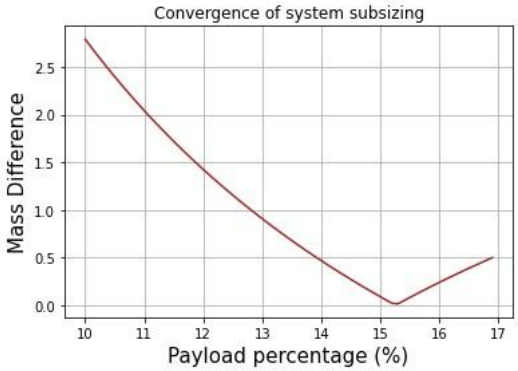

Figure 4: *Difference between the masses as a function of the payload percentage.*

From this plot, it can be concluded that convergence is achieved for a payload percentage of 15%. For this value, a value of 22 kg is achieved for the total mass. From this value, it can be concluded that the mass of propellant represents 2.85 kg, corresponding to 13% of the total mass and a dry mass of 15.85 kg, or 72% of the total system.

3.2 Hopping Trajectory

3.2.1 Results from Initial Guess

From the initial guess, it can be concluded that the whole trajectory is done in 4.7 s. The values for the maximum range of the hopper and the thrust-to-weight ratio can also be defined.

Regarding the maximum range, the initial guess allows us to conclude that for the maximum final horizontal velocity of 1 m/s, the maximum range of the hop must be 3.2 meters.

Concerning the thrust-to-weight ratio, and knowing that it must be greater than 1, from the initial guess, it can be concluded that if the ratio is close to 1, the mass of propellant used for a hop of 3.2 meters is greater. On the other hand, if the ratio is close to 2, the reaction wheels must output more torque for the hopper to turn faster, increasing the weight required for the hopper. For this reason, a value of 1.3 was chosen for the thrust-to-weight ratio 1.3. From this value, the maximum value of $\dot{m}_{max}$ can be calculated with the following equation

$$\dot{m}_{max} = \frac{twr \cdot m_{total} \cdot g_m}{Isp \cdot g_0}. \quad (45)$$

The initial guess also allows the estimation of the mass propellant consumption of each hop, using the equation

$$\frac{\Delta m}{m_{total}} = \frac{twr \cdot g_m}{I_{sp} \cdot g_0} t_{bal}. \quad (46)$$

Where t_{bal} is the duration of the ascent phase, as shown in Figure 3, from Equation 46, it can be concluded that the bigger the value of I_{sp}, the smaller the amount of propellant needed. Therefore, it is desirable to have the biggest value of I_{sp} possible.

3.3 Results from the Optimization

A gradient-based optimization was then attempted, using the GEKKO [29] Python library. The algorithm was run for a range of 1, 1.5, 2, 2.5, and 3.2 meters. For all these ranges, the algorithm was run until it converged to an optimal bang-bang solution, in which the thrust is maximum during the ascent phase. Regarding the reaction wheels, it was concluded that the algorithm converged when the relation.

$$\frac{Max(M_{rw})}{J_Z} = 1 \quad (47)$$

was respected. Meaning, the highest moment from the reaction wheels must equal the value of the moment of inertia of the hopper.

In Figure 5, the trajectories for all the ranges chosen can be seen. From this, it can be concluded that, as expected, all the trajectories resemble a ballistic trajectory.

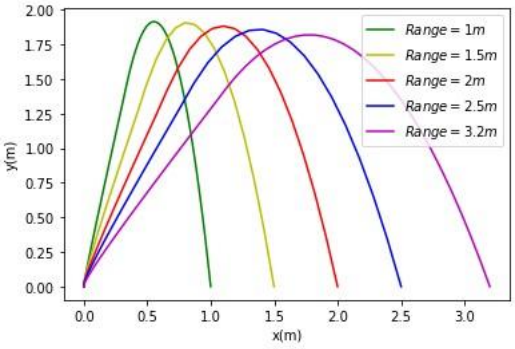

Figure 5: *Trajectories obtained*

In Figure 6, the pitch angle variations for all the trajectories can be seen. From this plot, it can be inferred that the pitch angle varies from 90º to a minimum of 78º, indicating that the hopper maintains its upward position throughout the trajectory.

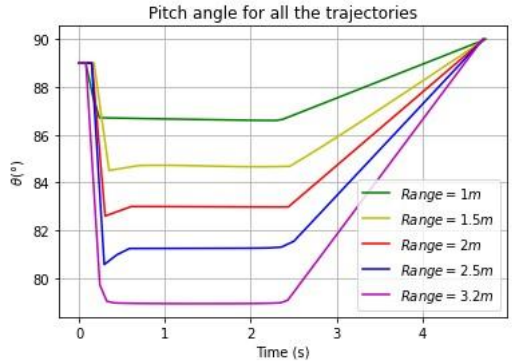

Figure 6: *Pitch angles for the trajectories obtained*

In Figure 7, it can be seen that the optimal bang-bang solution was obtained for each trajectory range and that the differences in the times of the ascent phase across ranges are small (the same conclusion holds with the initial guess).

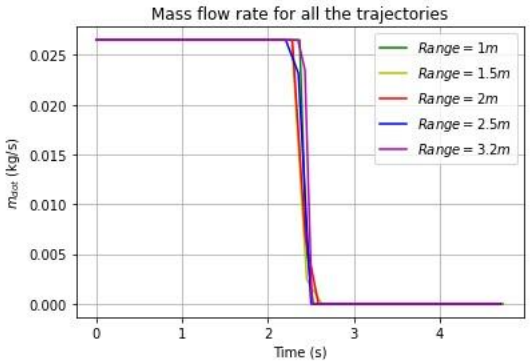

Figure 7: *Mass flow rate for all trajectories.*

In Figure 8, the profile of the reaction wheels divided by the moment of inertia can be seen. From this plot, it can be concluded that the trajectory with a range of 3.2 meters requires the most significant moment from the reaction wheels.

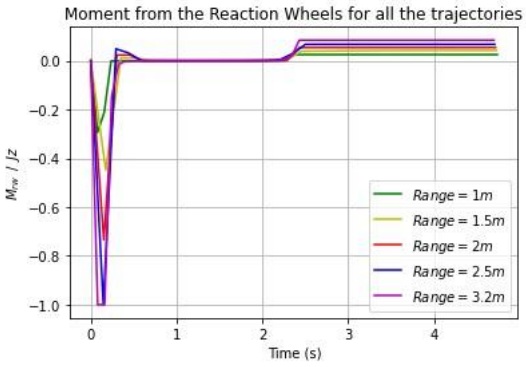

Figure 8: *Moment from the reaction wheels divided by the moment of Inertia for all the trajectories.*

From Figure 9, it can be concluded that for a trajectory with a range of 3.2 meters and an engine with an Isp of 243s, a propellant mass of 0.22% of the total mass is needed. It can also be concluded that the initial guess predicts a mass consumption lower than the actual value, of 0.211%.

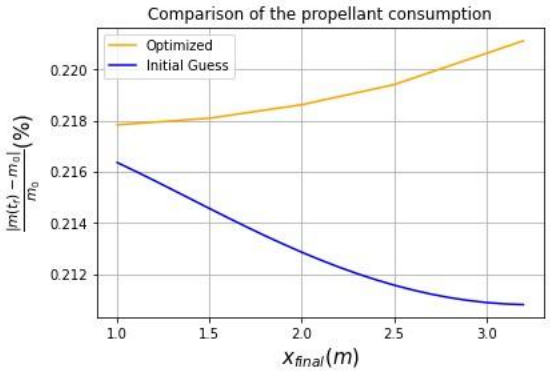

Figure 9: *Mass of propellant consumed for all trajectories.*

The difference in the trajectory obtained from the initial guess and the optimized one can be seen in Figure 10.

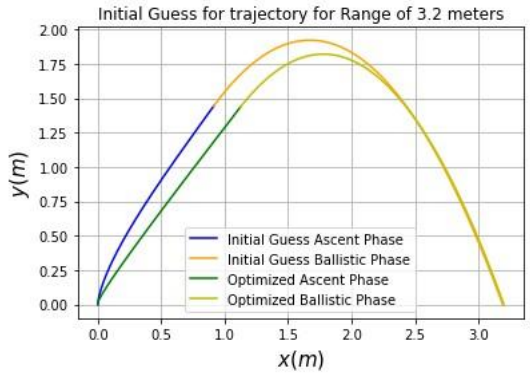

Figure 10: *Difference between initial guess and trajectories for a hop of 3.2m.*

3.4 Alternative trajectory

The trajectory, developed in section 3.2, assumes that the wheels of the hopper can bring the final horizontal velocity to 0 m/s from a maximum value of 1 m/s. However, an alternative method can be used to reach the end of the trajectory with a final horizontal velocity of 0 m/s, by using more energy from the reaction wheels and a larger mass of propellant for each hop. For this alternative method, the algorithm was run with the same initial conditions as stated in 2.4, with the constraint of the final horizontal velocity change to 0, in equation 43. The trajectory time was set to 5.5 s, and the algorithm was run over a range of 3.2 meters.

For this alternative method, the trajectory shown in Figure 11 does not resemble a ballistic trajectory. This is because, in the end phase of the trajectory, the hopper must have a vertical descent to land with a final horizontal velocity of 0 m/s.

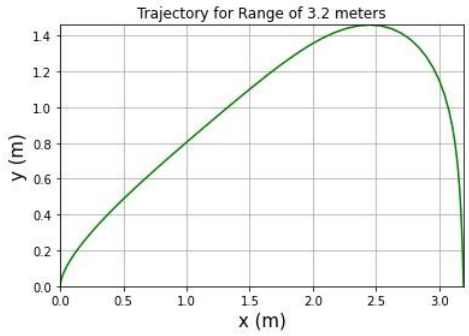

Figure 11: *Trajectory for the alternative method.*

Regarding the pitch angle, it also exhibits a larger variation, from a maximum of 126º to a minimum of 72º, as shown in Figure 12.

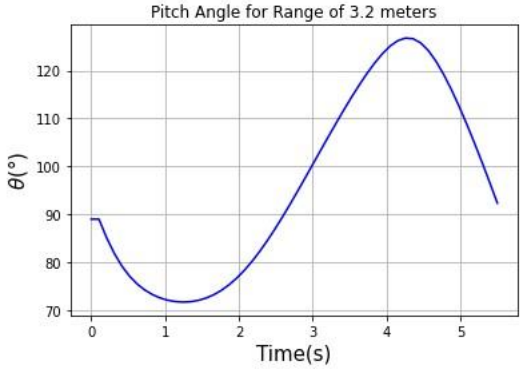

Figure 12: *Pitch angle for the alternative method.*

Regarding the control inputs, the algorithm does not converge to an optimal bang-bang solution, and instead has a more complex profile, as shown in Figure 13.

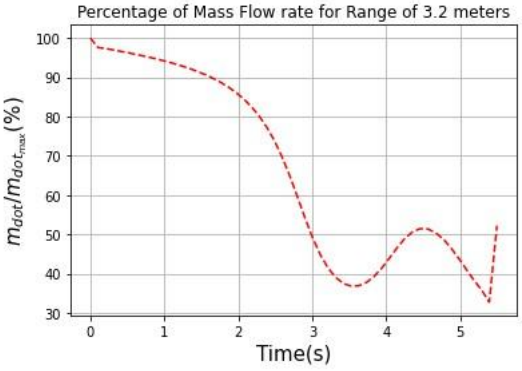

Figure 13: *Mass flow rate for the alternative method.*

The profile of the moment from the reaction wheels divided by the moment of inertia can also be seen in Figure 14. It can be concluded that the relation chosen in equation 47 still holds for this case.

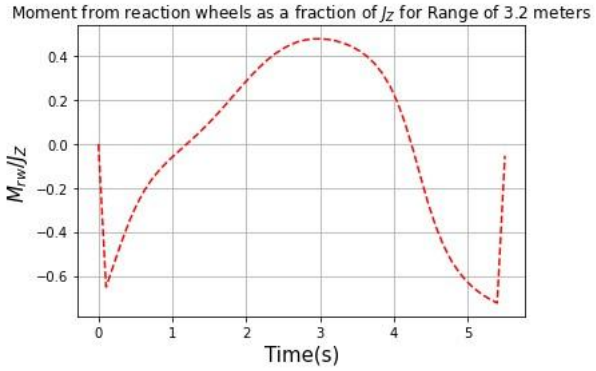

Figure 14: *Moment from the reaction wheels divided by the moment of inertia for the alternative method.*

With this alternative method, the mass propellant consumption per hop is 0.33% of the total mass. With this value, the required propellant mass for the mission increases. Following the methodology presented in 3.1, it can be concluded that, if this alternative method is used, convergence is achieved with a payload percentage of 12% and a hopper mass of 27.5 kg, an increase of 25% over the previous alternative.

4. Conclusions

This paper proposes the design of a lunar-propelled hopping system tailored for the exploration of lunar lava tubes.

The article analyzes in detail the preliminary sizing of the analyzed system following the methodology presented in [15].

The hopper's sizing is closely intertwined with its path-planning capabilities. Therefore, a detailed analysis of the hopper dynamics and its possible trajectory is presented.

Focusing on the hopping trajectory, it was also concluded that an optimization using the *GEKKO* library shows promising results. However, for this non-linear programming algorithm, a good initial guess is needed. The results from the initial guess were used to determine the Thrust-to-weight ratio and the maximum range of the trajectory for the optimization routine.

Based on the analysis, the concept of a lunar-propelled hopper could be a valuable addition to possible exploration systems venturing into lava tubes.

The work presented in this paper assumes that the hopper can be brought into the interior of the lunar lava tube using an external system. Future work would focus on studying and modeling the trajectory that would carry the hopper from the skylight to the interior of the lunar lava tube. For this trajectory, the landing phase must be included, and therefore, the initial guess will have six equations instead of 4.

As a contribution to the Aerospace community, the files that were used in the paper can be accessed at `https://github.com/JoaoGamboa/Moon-Hopper`.

Acknowledgements

The authors would like to thank the *Association aéronautique et astronautique de France* for the financial support. Moreover, they would like to thank the SACLAB Group at ISAE-SUPAERO for the support throughout the project.

References

[1] H. Kalita, A. Quintero Retis, A. Wissing, B. Haugh, *et al.*, "Mission concept: Cave and lava tube exploration on moon, mars and icy moons for eventual settlement", *Bulletin of the American Astronomical Society*, vol. 53, no. 4, p. 381, 2021.

[2] A. Legrand, J. Rimani, and S. Lizy-Destrez, "Robotic exploration of lunar lava tubes", 2021.

[3] R. Greeley, "Lava tubes and channels in the lunar marius hills", *The moon*, vol. 3, no. 3, pp. 289–314, 1971.

[4] T. Kaku, J. Haruyama, W. Miyake, A. Kumamoto, *et al.*, "Detection of intact lava tubes at Marius Hills on the moon by Selene (Kaguya) lunar radar sounder", *Geophysical Research Letters*, vol. 44, no. 20, pp. 10–155, 2017.

[5] R. Whittaker, U. Wong, H. Jones, S. Huber, *et al.*, "Exploration of planetary skylights and tunnels", Tech. Rep., 2014.

[6] L. Bessone, I. Carnelli, M. Fontaine, and F. Sauro, "Esa sysnova lunar caves challenge:

Ideas and technologies for a mission to lunar caves", in *52nd Lunar and Planetary Science Conference*, 2021, p. 1120.

[7] C. L. S. team, "Lunar caves cdf study - executive summary", ESA, 2022.

[8] A. P. Rossi, F. Maurelli, V. Unnithan, H. Dreger, *et al.*, "Daedalus - descent and exploration in deep autonomy of lava underground structures", Institut für Informatik, Tech. Rep. 21, 2021, p. 188.

[9] H. Kalita, R. T. Nallapu, A. Warren, and J. Thangavelautham, "Gnc of the spherex robot for extreme environment exploration on mars", *arXiv preprint arXiv:1701.07550*, 2017.

[10] W. B. White and D. C. Culver, *Encyclopedia of caves*. Academic Press, 2011.

[11] L. Beal, D. Hill, R. A. Martin, and J. Hedengren, *GEKKO Optimization Suite*. DOI: 10.3390/pr6080106.

[12] A. Fossa, G. Miceli, L. Beauregard, S. LizyDestrez, *et al.*, "Optimal control of trajectory of a reusable launcher in openmdao/dymos", in *Global Space Exploration Conference 2021*.

[13] P. F. Miaja, F. Navarro-Medina, D. G. Aller, G. León, *et al.*, "Robocrane: A system for providing a power and a communication link between lunar surface and lunar caves for exploring robots", *Acta Astronautica*, vol. 192, pp. 30–46, 2022.

[14] M. Persson, K. Anflo, A. Dinardi, and J. Bahu, "A family of thrusters for adnbased monopropellant lmp-103s", in *48th AIAA/ASME/SAE/ASEE Joint Propulsion Conference & Exhibit*, 2012, p. 3815.

[15] M. Isaji, I. Maynard, and B. Chudoba, "A new sizing methodology for lunar surface access systems", in *AIAA Scitech 2020 Forum*, 2020, p. 1775.

[16] B. Zandbergen, "Mass estimating relationships for manned lunar lander and ascent vehicle concept exploration", in *To the Moon and Beyond*, Deutsche Gesellschaft für Luft- und Raumfahrt (DGLR), 2008, pp. 1–8.

[17] J. Wertz, D. Everett, and J. Puschell, *Space Mission Engineering: The New SMAD*,
ser. Space technology library. Microcosm Press, 2011.

[18] Y. Gao, *Contemporary planetary robotics: an approach toward autonomous systems*. John Wiley and Sons, 2016.

[19] W. X. Michel, "Use and sizing of rocket hoppers for planetary surface exploration", Ph.D. dissertation, Massachusetts Institute of Technology, 2010.

[20] S.-P.
bibinitperiod D.-T. staff, "Margin philosophy for science assessment studies", ESA, 2012.

[21] N. Patel, R. Slade, and J. Clemmet, "The exomars rover locomotion subsystem", *Journal of Terramechanics*, vol. 47, no. 4, pp. 227–242, 2010.

[22] P. B. Jackson, "Overview of missile flight control systems", *Johns Hopkins APL technical digest*, vol. 29, no. 1, pp. 9–24, 2010.

[23] G. M. Siouris, *Missile guidance and control systems*. Springer Science and Business Media, 2004.

[24] E. M. Queen, *An Approach to Simulation of Extreme Conditions for a Planetary Lander*. National Aeronautics and Space Administration, Langley Research Center, 2001.

[25] T. Maeda, M. Otsuki, and T. Hashimoto, "Protection against overturning of a lunar planetary lander using a controlled landing gear", *Proceedings of the Institution of Mechanical Engineers, Part G: Journal of Aerospace Engineering*, vol. 233, no. 2, pp. 438–456, 2019. DOI: 10. 1177 / 0954410017742931. eprint: https://doi. Org/10.1177/0954410017742931.

[26] R. A. Martin, N. S. Gates, A. Ning, and J. D. Hedengren, "Dynamic optimization of high-altitude solar aircraft trajectories under station-keeping constraints", *Journal of Guidance, Control, and Dynamics*, vol. 42, no. 3, pp. 538–552, 2019.

[27] C. R. Harris, K. J. Millman, S. J. van der Walt, R. Gommers, *et al.*, "Array programming with NumPy", *Nature*, vol. 585, no. 7825, pp. 357–362, Sep. 2020. DOI: 10.1038/s41586020-2649-2.

[28] P. Virtanen, R. Gommers, T. E. Oliphant, M. Haberland, *et al.*, "SciPy1.0:FundamentalAlgorithms for Scientific Computing in Python", *Nature Methods*, vol. 17, pp. 261–272, 2020. DOI: 10.1038/s41592-019-0686-2.

[29] L. D. Beal, D. C. Hill, R. A. Martin, and J. D. Hedengren, "Gekko optimization suite", *Processes*, vol. 6, no. 8, p. 106, 2018.